SEGMENTING INTERNAL STRUCTURES IN 3D MR IMAGES OF THE BRAIN BY MARKOVIAN RELAXATION ON A WATERSHED BASED ADJACENCY GRAPH

T. Géraud†, J.-F. Mangin‡, I. Bloch† and H. Maître†

†Département Images, École Nationale Supérieure des Télécommunications
46, rue Barrault, 75634 Paris Cedex 13, France
e-mail geraud@ima.enst.fr
‡Service Hospitalier Frédéric Joliot, Commissariat à l'Énergie Atomique, Orsay, France

ABSTRACT

In this paper we present a fast stochastic method aiming at segmenting cerebral internal structures in 3D magnetic resonance images. An original method introducing context permits us to obtain reliable radiometric characteristics even for hardly discriminable brain structures. Segmentation is formulated as the labeling of a region adjacency graph. The graph is constructed by an extension to 3D of the watershed algorithm and the labeling is performed using a Markovian relaxation process. This leads to consistent results with a very low computational burden.

1. INTRODUCTION

The number of applications of magnetic resonance imaging (MRI) for non-invasive examination of internal cerebral structures is steadily growing. Important medical issues are, for instance, to provide an anatomical reference for functional studies, or to find automatically the straight path from a point external to the head towards a pathological region in the brain which minimizes surgical risks. The use of MR anatomical images of the patient presents advantages over atlases which have to be deformed to fit the functional data: the variability between the patient brain structure location and shape and the atlas information [10] can be high. This leads to imprecise results, or even to false results in some pathological cases when structures are too different from their atlas model.

In order to obtain reliable anatomical information, a precise 3D segmentation of brain structures in the MR images is needed. While the segmentation of cerebro-spinal fluid located in sulci (S) and ventricles (V), of white matter (W) and of gray matter (G) is widely addressed, other internal structures (OIS) such as caudate nuclei, putamen or thalamus have received little attention until now [7][13] (these key anatomical features are indicated in figure 1). This paper is a contribution to the automation of their delineation.

The proposed method associates an original, robust estimation of class statistical parameters described in section

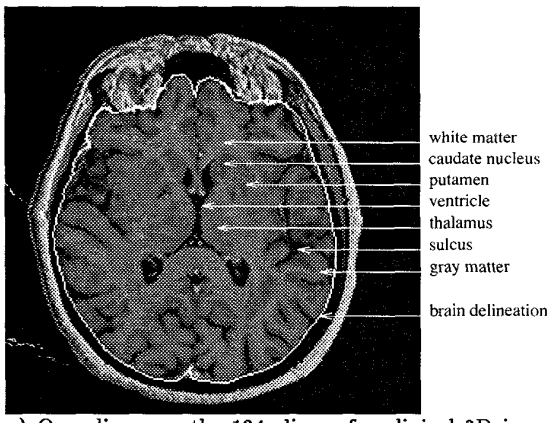

a) One slice over the 124 slices of a clinical 3D image; the slice thickness is 1.35mm and the in-plane resolution is 1mm by 1mm for 256x256 points.

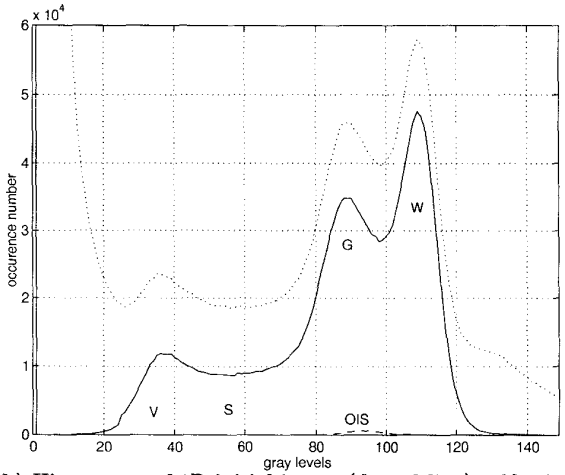

b) Histograms of 3D initial image (dotted line), of brain volume (solid line), of OIS manually delineated (dashed line).

Figure 1: MRI radiometric data.

This work was supported by the French Ministry for Research (MESR)

2 and a Markovian relaxation on an over-segmentation adjacency graph based on morphological information described in section 3. Such an approach leads to a very low computational burden applied to 3D images.

2. RADIOMETRIC PARAMETER ESTIMATION

2.1. Introduction

We characterize the statistical radiometric behavior of different brain tissues using their gray-level mean and variance. A major impediment is that these characteristics do not provide a good discrimination of OIS relative to white and gray matter: this can be seen from the histograms shown in figure 1b. We observe that, even on the brain histogram, which is more pertinent to this problem than the whole 3D image histogram, OIS radiometric characteristics are hidden by those of white and gray matter. Therefore, the commonly used automatic methods fail in discriminating them and usually label OIS either as white matter or as gray matter [8].

In this section, we propose a fully automatic procedure able to estimate reliable parameters for all these different cerebral structures. Until now, this task was performed on regions of interest delineated manually by a physician [4]; the results were not statistically reliable due to the low number of voxels taken into account and due to the bias introduced by human subjectivity. The method that we have developed introduces contextual information in the radiometric analysis. Based on a rough initial classification of the brain image, the method relies on an automatic analysis of the evolution of gray-level statistics on each side of the interface between two image classes.

2.2. Contextual approach

Let us consider an initial class image (figure 2a). A distance map to all class borders, that is a generalized Voronoï diagram, is calculated (figure 2b) using the chamfer transform [11]. In addition to propagating distances, we also propagate the class label defining the border from which the distance is measured (the resulting class image is depicted in figure 2c). Thus we know, for each point in the image, its *a priori* class label as given by the initial classification, and we have found the distance from its class boundary as well as a label indicating to which neighbor class this point is closest.

We can then define both sides of an "interface" between two classes labeled i and j by the points whose initial label is i (respectively j) and whose closest neighbor label is j (respectively i). So, each point can be characterized as belonging to one particular side of a unique interface and by its distance from the interface frontier. Figure 2d shows the interface boundaries (white solid line) and the frontiers (white dashed lines); the gray-levels indicate the chamfer distance behaviour.

This contextual information will serve in discriminating OIS from white and gray matter and in getting reliable statistics.

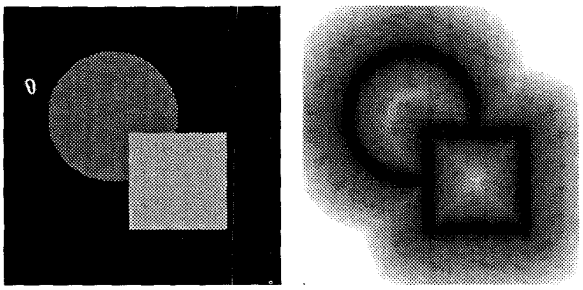

a) initial class image b) distance image

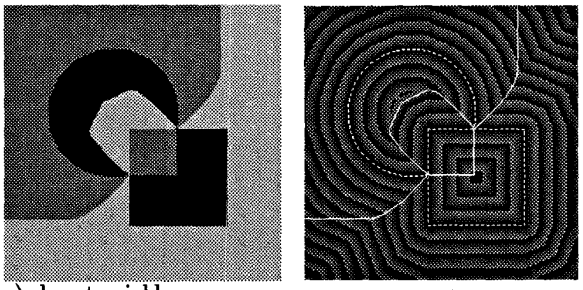

c) closest neighbor class image d) resulting interfaces

Figure 2: Phantom image and definition of "interfaces"

2.3. Data preprocessing

As the only region of interest in the 3D MR acquisition image is the brain itself, the first step of data preprocessing consists of brain segmentation [6]. We use connected component labeling and morphological operators [9] whose structuring elements are balls constructed with anisotropic chamfer distance transform adapted to the voxel sizes of the MR image. The resulting brain contour and the histogram of the brain volume are shown in figure 1.

An automated algorithm such as a fuzzy c-means classifier [1] typically provides four classes from this 3D brain image. The first corresponds to the image background, outside the brain mask, the second to the cerebro-spinal fluid (CSF) located both in sulci and in ventricles, the third to the sum of gray matter and mis-classified OIS, and the last to white matter. The use of morphological opening allows us to split the CSF class in two parts: sulci and ventricles. We finally use order filters to softly regularize the five classes before proceeding with the contextual analysis described in section 2.2.

2.4. Parameter estimation

Let us consider an interface between two classes. For each set of points having the same discrete distance on one side of this interface, we calculate the radiometric mean and variance from the initial gray-scale image. Thus, we can analyse the evolution of gray-level statistics between two brain structures. The points which are close to the interface frontier (small distances) may be affected by the following two phenomena. Either they may be misclassified in the initial classification and thus they are not properly taken into account for the statistics, or they may be affected by

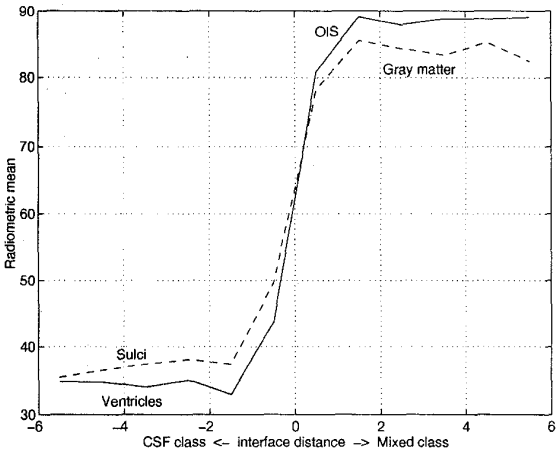

Figure 3: Radiometric mean estimation. Our method efficiently provides a discrimination between OIS and gray matter; note that the evolution of gray-level mean for CSF shows that sulcus fluid suffers from important partial volume effects in comparison with ventricle fluid.

partial volume effects which shift the statistics. On the contrary, when the distance to the interface frontier grows, it ensures that the corresponding points, far from class boundaries, are correctly classified and composed of pure tissue only. We finally get reliable and robust statistics as they are computed on pure tissue areas for all classes.

OIS are finally detected as the points misclassified as gray matter belonging to the interface between ventricles and gray matter, whereas "true" gray matter points belong to the interface between sulci and gray matter. To validate our method, we have manually segmented the different brain structures and verified that the statistics provided by our method were correct. The conditional histogram of OIS is shown in figure 1b and the radiometric mean effectively correspond to the result depicted in figure 3.

The statistical parameters provided during this step allow for the construction of reliable potentials in the relaxation process proposed in the following.

3. INTERNAL STRUCTURE SEGMENTATION

3.1. Introduction

Markovian relaxation [2] is a powerful approach for combining both local statistical information and various *a priori* knowledge such as spatial consistency. Its major drawback is that a stochastic relaxation performed on a 3D image lattice is computationally very expensive because it requires an important number of iterations to give good results and because each iteration concerns a huge number of voxels (about 8 million for high-resolution MRI). The key feature of our method is that it relies on an initial over-segmentation [5], [3]. The problem is then formulated as a consistent labeling of regions: the sites to be classified are thus regions and not voxels. This drastic decrease of the number of sites allows the use of simulated annealing with very reasonable computational cost.

3.2. Over-segmentation and graph construction

We aim at obtaining an over-segmentation with the constraint that the contours of the structures of interest are a subset of the over-segmentation contours. It can be achieved by using a 3D analogy to the watershed concept [12], which subdivides the brain image into a set of disjoint regions called catchment basins, whose separating surface is the "crest" surface of the gradient. Thus voxels are clustered together based on their spatial proximity and their radiometric homogeneity and the watershed is exhibited as a surface of one voxel thickness separating all the basins. To reduce the number of basins, which is equal to the number of minima in the gradient image, a morphological closure is applied to the gradient image before applying the watershed algorithm. The strength of the closure depends on the structuring element size: the number of minima decreases when the ball radius grows (for small radii, only very local minima are suppressed).

The resulting over-segmentation corresponds to a tessellation of the brain volume which can be modelized by a region adjacency graph where nodes correspond to basins and arcs to adjacencies between basins. Nodes and arcs are endowed with various attributes. Information located in the graph nodes is related to the basins: for instance, the basin volume ($vol(s)$) in number of voxels, the gray-level mean (y_s) calculated over the basin voxels, the coordinates of the basin mass centre, and so forth. A link between two graph nodes indicates that the two corresponding basins are neighbors. Information related to the basin connectivity is located on the graph adjacency links, for instance, the surface ($surf(s,q)$) in number of voxels of the watershed frontier between the two neighbor basins.

3.3. Markovian relaxation

The adjacency graph is endowed with a MRF structure: the field sites are the graph nodes and clique systems are defined from the graph neighborhood structure. The use of potential functions associated with different clique types is a powerful tool for incorporating the knowledge about the internal brain structure model. The graph labeling issue is then formulated as a global energy minimization problem, which can be performed with simulated annealing.

Let us denote by y the observation. It is composed of characteristics located in graph nodes and derivated directly from the gray-scale image to be classified; let y_s be the characteristics of site s (in our application, the radiometric mean of the basin voxels). Let us now denote by x a realisation of the random field associated with the graph labeling; $x_s = i$ means that site s belongs to class i for this realisation. We are looking for the realisation s which maximizes the *a posteriori* probability density function $p(x|y)$. By Bayes' theorem, we have $p(x|y) = p(y|x)p(x)/p(y)$ where $p(y|x)$ is the conditional density of the observation given the labeling and $p(x)$ the *a priori* density of the labeling.

As we model the graph as a Markov random field, we have $p(x_s|x_q, \text{ all } q \neq s) = p(x_s|x_q, q \in N_s)$ where N_s is the neighborhood of site s. According to the Hammersley-Clifford theorem, if no realisation has zero probability, the density of x is then given by a Gibbs density: $p(x) = \frac{1}{Z}\exp\{-\sum_C V_C(x)\}$ where Z is a normalizing constant

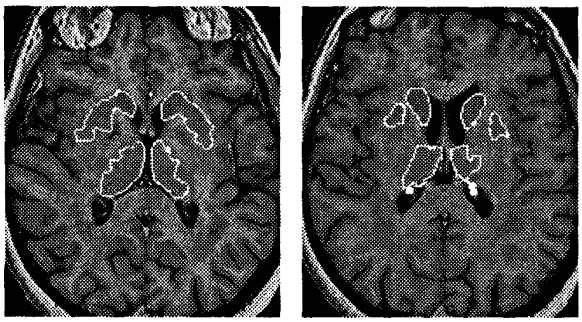

Figure 4: Segmentation results on two slices.

and C a clique. We have $V_C(x) = \sum_s V_C(x_s)$ but we only take into account two-site cliques in our application (a one-site clique potential could be used to introduce fuzzy *a priori* spatial knowledge: some structures are located more deeply in the brain than others, in the left hemisphere or in the right one, etc.). We set those clique potentials to modelize anatomical relationships between brain structures through a Potts model. To that end, a matrix P contains potential values which indicate how certain class neighbors are favored (negative potentials) or disfavored (positive ones). Thus we have
$V_C(x_s) = surf(s,q)P_{x_s,x_q}$, if $C = \{s,q\}, 0$ otherwise.

We model the conditional density as a white Gaussian process which parameters, the radiometric mean μ_i and variance σ_i for each class label i, are directly derived from the first estimation step (section 2.4). So, we get the following data attachment term
$p(y|x) = \exp\{-vol_s \sum_s \frac{1}{2\sigma_{x_s}^2}(y_s - \mu_{x_s})^2\}$.

A stochastic relaxation is then performed with the classical Metropolis algorithm.

3.4. Results and discussion

The combination of local properties and contextual information guarantees a very strong coherence of the final result with the scene model: in figure 3, we see that OIS have been successfully located in the 3D MR image by our method. Unfortunately, the watershed algorithm does not provide a very proper delineation of structures due to the influence of the morphological closing that precedes this step. Our results can be significantly improved by the use of an over-segmentation process more suited to thin shapes.

The simulated annealing performed on the about 32000 regions obtained with the watershed algorithm converges in about 500 iterations which takes less than 1 minute of calculations on a Unix workstation (Sun Sparc Center 2000) whereas a classical Markovian relaxation over the 256x256x124 voxels of the 3D magnetic resonance image takes several hours. The whole process (initial classification, radiometric parameter estimation, gradient calculation and closing, watershed algorithm, graph construction, and relaxation) takes less than 5 minutes.

Segmentation of hardly discriminable objects is now possible by the combination of low and high-level techniques that we have extended to 3D. Future work concerns a refinement and a systematization of this method permitting a recognition of the entire internal structure of the brain.

4. REFERENCES

[1] K.S. Al-Sultan and S.Z. Selim, "A Global Algorithm for the Fuzzy Clustering Problem," *Pattern Recognition*, vol. 26, no. 9, pp. 1357-1361, 1993.

[2] S. Geman and D. Geman, "Stochastic Relaxation, Gibbs Distribution, and the Bayesian Restoration of Images," *IEEE Trans. on Pattern Anal. Machine Intell.*, vol.6, no.6, pp.721-741, November 1984.

[3] M.W. Hansen and W.E. Higgins, "Watershed-Driven Relaxation Labeling for Image Segmentation," *IEEE Int. Conf. on Image Processing*, Austin, Texas, pp. 460-463, November 1994.

[4] W.E. Higgins, W.L. Sharp, M.W. Hansen, and J.M. Reinhardt, "A Graphical User Interface System for 3D Medical Image Analysis," *SPIE Medical Imaging 94*, vol. 2164, pp. 95-106, February 1994.

[5] I.Y. Kim and H.S. Yang, "Efficient Image Labeling Based on Markov Random Field and Backpropagation Network," *Pattern Recognition*, vol. 26, no. 11, pp. 1695-1707, 1993.

[6] J.-F. Mangin, V. Frouin, I. Bloch, J. Régis, and J. Lopez-Krahe, "Automatic Construction of an Attributed Relational Graph Representing the Cortex Topography using Homotopic Transformations," *SPIE Mathematical Methods in Medical Imaging* III, vol.2299, pp.110-121, San Diego, July 1994.

[7] G. Mittelhausser and F. Kruggel, "Fast Segmentation of Brain Magnetic Resonance Tomograms," *Conf. on Computer Vision, Virtual Reality and Robotics in Medicine*, Springer Ed., pp.237-241, Nice, France, April 1995.

[8] T.N. Pappas, "An Adaptative Clustering Algorithm for Image Segmentation," *IEEE Trans. on Signal Processing*, vol.40, no.4, pp.901-914, April 1992.

[9] J. Serra, *Image Analysis and Mathematical Morphology*, Academic Press, 1982.

[10] J. Talairach and P. Tournoux, *Co-Planar Stereotaxic Atlas of the Human Brain - 3D Proportional System: an Approach to Cerebral Imaging*, Thieme Medical Publisher, Inc., Georg Thieme Verlag, 1990.

[11] B.J.H. Verwer, "Local Distances for Distance Transformations in Two or Three Dimension," *Pattern Recognition Letters*, vol.12, pp.671-682, 1991.

[12] L. Vincent and P. Soille, "Watersheds in Digital Spaces: An Efficient Algorithm Based on Immersion Simulations," *IEEE Trans. Pattern Anal. Machine Intell.*, vol.13, no.6, pp.583-598, June 1991.

[13] K.L. Vincken, A.S.E. Koster, and M.A. Viergever, "Probabilistic Hyperstack Segmentation of MR Brain Data," *Conf. on Computer Vision, Virtual Reality and Robotics in Medicine*, Springer Ed., pp.351-357, Nice, France, April 1995.